Band-Structure Trend in Hole-Doped Cuprates and Correlation with $T_{c\,\max}$

E. Pavarini, I. Dasgupta,* T. Saha-Dasgupta,† O. Jepsen, and O. K. Andersen
Max-Planck-Institut für Festkörperforschung, D-70506 Stuttgart, Germany
(Received 4 December 2000; published 10 July 2001)

By calculation and analysis of the bare conduction bands in a large number of hole-doped high-temperature superconductors, we have identified the range of the intralayer hopping as the essential, material-dependent parameter. It is controlled by the energy of the axial orbital, a hybrid between Cu $4s$, apical-oxygen $2p_z$, and farther orbitals. Materials with higher $T_{c\,\max}$ have larger hopping ranges and axial orbitals more localized in the CuO_2 layers.

DOI: 10.1103/PhysRevLett.87.047003 PACS numbers: 74.25.Jb, 74.62.Bf, 74.62.Fj, 74.72.–h

The mechanism of high-temperature superconductivity (HTSC) in the hole-doped cuprates remains a puzzle [1]. Many families with CuO_2 layers have been synthesized and all exhibit a phase diagram with T_c going through a maximum as a function of doping. The prevailing explanation is that at low doping, superconductivity is destroyed with rising temperature by the loss of phase coherence, and at high doping by pair breaking [2]. For the *materials* dependence of T_c at optimal doping, $T_{c\,\max}$, the only known, but not understood, systematics is that for materials with multiple CuO_2 layers, such as $HgBa_2Ca_{n-1}Cu_nO_{2n+2}$, $T_{c\,\max}$ increases with the number of layers, n, until $n \sim 3$. There is little clue as to why for n fixed, $T_{c\,\max}$ depends strongly on the family, e.g., why for $n = 1$, $T_{c\,\max}$ is 40 K for La_2CuO_4 and 85 K for $Tl_2Ba_2CuO_6$, although the Néel temperatures are fairly similar. A wealth of structural data has been obtained, and correlations between structure and T_c have often been looked for as functions of doping, pressure, uniaxial strain, and family. However, the large number of structural and compositional parameters makes it difficult to find what besides doping controls the superconductivity. Recent studies of thin epitaxial $La_{1.9}Sr_{0.1}CuO_4$ films concluded that the distance between the charge reservoir and the CuO_2 plane is the key structural parameter determining the normal state and superconducting properties [3].

Most theories of HTSC are based on a Hubbard model with *one* Cu $d_{x^2-y^2}$-like orbital per CuO_2 unit. The one-electron part of this model is, in the $\mathbf{k}$ representation,

$$\varepsilon(\mathbf{k}) = -2t(\cos k_x + \cos k_y) + 4t' \cos k_x \cos k_y - 2t''(\cos 2k_x + \cos 2k_y) + \ldots, \quad (1)$$

with $t, t', t'', \ldots$ denoting the hopping integrals (≥ 0) on the square lattice (Fig. 1). First, only t was taken into account, but the consistent results of local-density approximation (LDA) band-structure calculations [4] and angle-resolved photoemission spectroscopy (for overdoped, stripe-free materials) [5] have led to the current usage of including also t', with $t'/t \sim 0.1$ for La_2CuO_4 and $t'/t \sim 0.3$ for $YBa_2Cu_3O_7$ and $Bi_2Sr_2CaCu_2O_8$, whereby the constant-energy contours of expression (1) become rounded squares oriented in, respectively, the [11] and [10] directions. It is conceivable that the materials dependence enters the Hamiltonian primarily via its one-electron part (1) and that this dependence is captured by LDA calculations, but it needs to be filtered out.

The LDA band structure of the best known, and only stoichiometric optimally doped HTSC, $YBa_2Cu_3O_7$, is more complicated than what can be described with the t-t' model. Nevertheless, careful analysis has shown [4] that the *low*-energy *layer*-related features, which are the only generic ones, can be described by a *nearest*-neighbor tight-binding model with *four* orbitals per layer (Fig. 1), Cu $3d_{x^2-y^2}$, O_a $2p_x$, O_b $2p_y$, and Cu $4s$, with the interlayer hopping proceeding via the diffuse Cu $4s$ orbital whose energy ε_s is several eV above the conduction band. Also the intralayer hoppings $t', t'', \ldots$, beyond nearest neighbors in (1) proceed via Cu s. The constant-energy contours, $\varepsilon_i(\mathbf{k}) = \varepsilon$, of this model could be expressed as [4]

$$1 - u - d(\varepsilon) + (1 + u)p(\varepsilon) = \frac{v^2}{1 - u + s(\varepsilon)} \quad (2)$$

in terms of the coordinates $u \equiv \frac{1}{2}(\cos k_x + \cos k_y)$ and $v \equiv \frac{1}{2}(\cos k_x - \cos k_y)$, and the quadratic functions $d(\varepsilon) \equiv (\varepsilon - \varepsilon_d)(\varepsilon - \varepsilon_p)/(2t_{pd})^2$ and $s(\varepsilon) \equiv (\varepsilon_s - \varepsilon) \times (\varepsilon - \varepsilon_p)/(2t_{sp})^2$, which describe the coupling of $O_{a/b}\,p_{x/y}$ to, respectively, Cu $d_{x^2-y^2}$ and Cu s. The term proportional to $p(\varepsilon)$ in (2) describes the admixture of $O_{a/b}\,p_z$ orbitals for dimpled layers and actually extends the four-orbital model to a six-orbital one [4]. For ε

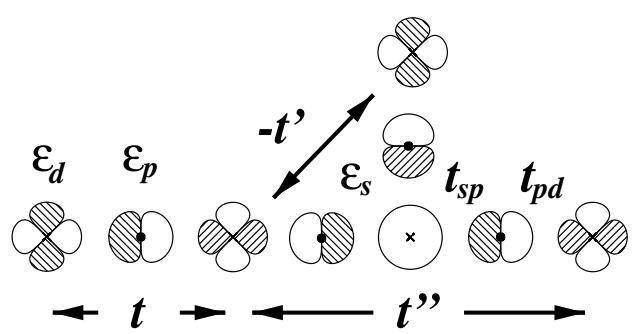

FIG. 1. Relation between the one-orbital model ($t, t', t'', \ldots$) and the nearest-neighbor four-orbital model [4] ($\varepsilon_d - \varepsilon_p \sim 1$ eV, $t_{pd} \sim 1.5$ eV, $\varepsilon_s - \varepsilon_p \sim 4$–$16$ eV, $t_{sp} \sim 2$ eV).

near the middle of the conduction band, $d(\varepsilon)$, $s(\varepsilon)$, and $p(\varepsilon)$ are positive, and the energy dependence of $d(\varepsilon)$ may be linearized ($\dot{d} > 0$), while those of $s(\varepsilon)$ and of $p(\varepsilon)$ may be neglected. The bilayer bonding and antibonding subbands have ε_s values split by $\mp t_{ss}^{\perp}$. Now, if ε_s were infinitely far above the conduction band, or t_{sp} vanishingly small, the right-hand side of (2) would vanish, with the result that the constant-energy contours would depend only on u. The dispersion of the conduction band near the Fermi level would thus be that of the one-orbital model (1) with $t = (1 - p)/4\dot{d}$ and $t' = t'' = 0$. For realistic values of ε_s and t_{sp}, the conduction band attains Cu s character proportional to v^2, thus vanishing along the nodal direction, $k_x = k_y$, and peaking at $(\pi, 0)$, where it is of order 10%. The repulsion from the Cu s band lowers the energy of the Van Hove singularities and turns the constant-energy contours towards the [10] directions. In a multilayer material, this same v^2 dependence pertains to the interlayer splitting caused by $t_{ss}^{\perp}$. In order to go from (2) to (1), $1/(1 - u + s) \equiv 2r/(1 - 2ru)$ was expanded in powers of $2ru$, where $r \equiv \frac{1}{2}/(1 + s)$. This provided explicit expressions, such as $t = [1 - p + o(r)]/4\dot{d}$, $t' = [r + o(r)]/4\dot{d}$, and $t'' = \frac{1}{2}t' + o(r)$, for the hopping integrals of the one-orbital model in terms of the parameters of the four(six)-orbital model and the expansion energy $\sim\varepsilon_F$. Note that all intralayer hoppings beyond nearest neighbors are expressed in terms of the *range* parameter r. Although one may think of r as t'/t, this holds only for flat layers and when $r < 0.2$. When $r > 0.2$, the series (1) must be carried beyond t''. Dimpling is seen not to influence the range of the intralayer hopping, but to reduce t through admixture of $O_{a/b}\, p_z$. In addition, it also reduces t_{pd}.

Here, we generalize this analysis to all known families of HTSC materials using a new muffin-tin-orbital (MTO) method [6] which allows us to construct minimal basis sets for the low-energy part of an LDA band structure with sufficient accuracy that we can extract the materials dependence. This dependence we find to be contained solely in ε_s, which is now the energy of the *axial* orbital, a hybrid between Cu s, Cu d_{3z^2-1}, apical-oxygen $O_c\, p_z$, and farther orbitals on, e.g., La or Hg. The range, r, of the intralayer hopping is thus controlled by the structure and chemical composition *perpendicular* to the CuO_2 layers. It turns out that the materials with the larger r (lower ε_s) tend to be those with the higher observed values of $T_{c\,\max}$. In the materials with the highest $T_{c\,\max}$, the axial orbital is almost pure Cu $4s$. It should be noted that r describes the *shape* of the noninteracting band in a 1 eV range around the Fermi level, whose accurate position is unknown because we make no assumptions about the remaining terms of the Hamiltonian, inhomogeneities, stripes, etc.

Figure 2 shows the LDA bands for the single-layer materials La_2CuO_4 and $Tl_2Ba_2CuO_6$. Whereas the high-energy band structures are complicated and very different, the low-energy conduction bands shown by dashed lines contain the generic features. Most notably, the dispersion

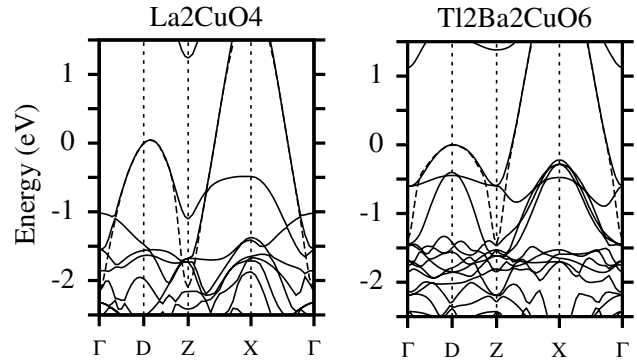

FIG. 2. LDA bands (solid lines) and Cu $d_{x^2-y^2}$-like conduction band (dashed line). In the bct structure, $\Gamma = (0,0,0)$, $D = (\pi,0,0)$, $Z = (2\pi,0,0) = (0,0,2\pi/c)$, and $X = (\pi,\pi,0)$.

along ΓDZ is suppressed for $Tl_2Ba_2CuO_6$ relatively to La_2CuO_4, whereas the dispersion along ΓXZ is the same. This is the v^2 effect. The low-energy bands were calculated variationally with a single Bloch sum of Cu $d_{x^2-y^2}$-like orbitals constructed to be correct at an energy near half filling. Hence, these bands agree with the full band structures to linear order and head towards the pure Cu $d_{x^2-y^2}$ levels at Γ and Z, extrapolating across a multitude of irrelevant bands. This was explained in Ref. [6]. Now, the hopping integrals $t, t', t'', \ldots$ may be obtained by expanding the low-energy band as a Fourier series, yielding $t = 0.43$ eV in both cases, $t'/t = 0.17$ for La_2CuO_4 and 0.33 for $Tl_2Ba_2CuO_6$, plus many further interlayer and intralayer hopping integrals [7].

That all these hopping integrals and their materials dependence can be described with a generalized four-orbital model is conceivable from the appearance of the conduction-band orbital for La_2CuO_4 in the xz plane (Fig. 3). Starting from the central Cu atom and going in the x direction, we see $3d_{x^2-y^2}$ antibond to neighboring $O_a\, 2p_x$, which itself bonds to $4s$ and antibonds to $3d_{3z^2-1}$ on the next Cu. From here, and in the z direction, we see $4s$ and $3d_{3z^2-1}$ antibond to $O_c\, 2p_z$, which itself bonds to La orbitals, mostly $5d_{3z^2-1}$. For $Tl_2Ba_2CuO_6$ we find about the same amount of Cu $3d_{x^2-y^2}$ and $O_{a/b}\, 2p_{x/y}$ character, but more Cu $4s$, negligible Cu $3d_{3z^2-1}$, much less $O_c\, 2p_z$, and Tl $6s$ instead of La $5d_{3z^2-1}$ character. In $Tl_2Ba_2CuO_6$ the axial part of the conduction-band orbital is thus mainly Cu $4s$.

Calculations with larger basis sets than one MTO per CuO_2 now confirm that, in order to localize the orbitals so much that only nearest-neighbor hoppings are essential, one needs to add *one* orbital, Cu axial, to the three standard orbitals. The corresponding four-orbital Hamiltonian is therefore the one described above in Fig. 1 and Eq. (2). Note that we continue to call the energy of the axial orbital ε_s and its hopping to $O_a\, p_x$ and $O_b\, p_y$ t_{sp}. Calculations with this basis set for many different materials show that, of all the parameters, only ε_s varies significantly [7]. This variation can be understood in terms of the couplings between the constituents of the axial orbital sketched in the

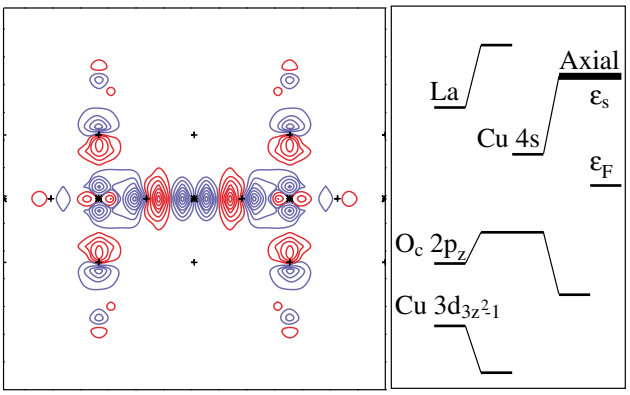

FIG. 3 (color). Left: MTO describing the Cu $d_{x^2-y^2}$-like conduction band in La_2CuO_4. The plane is perpendicular to the layers and passes through Cu, O_a, O_c, and La. Right: schematic diagram giving the energy ε_s of the *axial* orbital in terms of the energies of its constituents and their couplings.

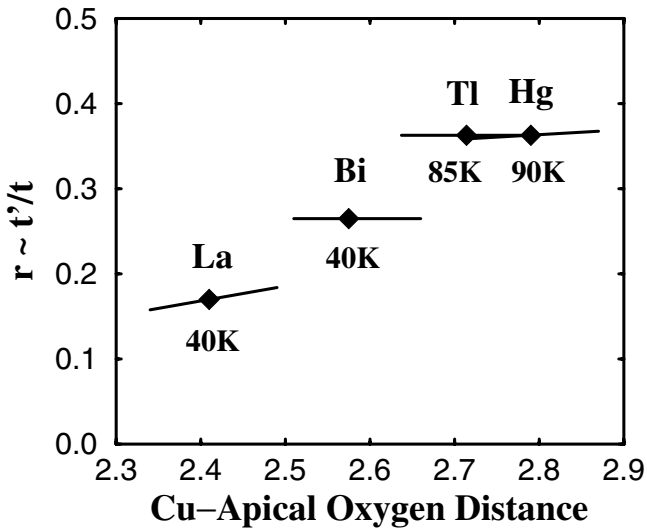

FIG. 4. Calculated range parameter, r, for single-layer materials vs the distance (in Å) between Cu and O_c. The lines result from rigid displacements of O_c.

right-hand panel of Fig. 3: We first form the appropriate O_c p_z-like five-atom hybrid Cu d_{3z^2-1}-2O_c p_z-2La with the energy [7]

$$\varepsilon_c = \varepsilon_{\bar{c}} + \left(1 + \frac{t_{sc}}{t_{sp}}\frac{t_{pz^2}}{t_{cz^2}}\right)^2 \frac{4\bar{r}t_{cz^2}^2}{\varepsilon_F - \varepsilon_{z^2}} - \frac{t_{c\mathrm{La}}^2}{\varepsilon_{\mathrm{La}} - \varepsilon_F} \tag{3}$$

and then couple this to the Cu s orbital to yield the axial-orbital energy: $\varepsilon_s = \varepsilon_{\bar{s}} + 2t_{sc}^2/(\varepsilon_F - \varepsilon_c)$. Here, $\varepsilon_{\bar{s}}$ and $\varepsilon_{\bar{c}}$ denote the energies of the pure Cu s and O_c p_z orbitals, and t_{sc} denotes the hopping between them. The energy of Cu d_{3z^2-1} is ε_{z^2} and its hopping integrals to $O_{a/b}p_{x/y}$ and $O_c p_z$ are, respectively, t_{pz^2} and t_{cz^2}. In deriving Eqs. (2) and (3), we have exploited that $t_{pz^2}^2/t_{sp}^2 \ll \frac{\varepsilon_F - \varepsilon_{z^2}}{\varepsilon_{\bar{s}} - \varepsilon_F}$ and that $t_{pd}^2/t_{sp}^2 \ll \frac{\varepsilon_F - (\varepsilon_p + \varepsilon_d)/2}{(\varepsilon_p + \varepsilon_s)/2 - \varepsilon_F}$. Although specific for La_2CuO_4, Eq. (3) is easy to generalize.

In Fig. 4 we plot the r values for single-layer materials against the distance $d_{\text{Cu-O}_c}$ between Cu and apical oxygen. r increases with $d_{\text{Cu-O}_c}$ because ε_s is lowered towards ε_F when the hoppings t_{cz^2} and t_{sc} from O_c p_z to Cu d_{3z^2-1} and Cu s are weakened. Since $t_{cz^2} \propto d_{\text{Cu-O}_c}^{-4}$ and $t_{sc} \propto d_{\text{Cu-O}_c}^{-2}$, increasing the distance suppresses the Cu d_{3z^2-1} content, which is important in La_2CuO_4, but negligible in $Tl_2Ba_2CuO_6$ and $HgBa_2CuO_4$. This is also reflected in the slopes of the lines in Fig. 4 which, for each material, give r vs $d_{\text{Cu-O}_c}$. The strong slope for La_2CuO_4 explains the strained-film results [3], provided that r correlates with superconductivity. That the Bi point does not fall on the La line is an effect of Bi being different from La: Bi $6p_z$ couples stronger to O_c $2p_z$ than does La $5d_{3z^2-1}$. The figure shows that upon reaching $HgBa_2CuO_4$, r is saturated, $\varepsilon_s \sim \varepsilon_{\bar{s}}$, and the axial orbital is almost pure Cu $4s$.

Figure 4 hints that for single-layer materials r might correlate with the observed $T_{c\,\max}$, but the experimental uncertainties of both $T_{c\,\max}$ and the structural parameters are such that we need better statistics. We therefore plot the observed $T_{c\,\max}$ against the calculated r values for nearly all hole-doped HTSCs in Fig. 5. For the single-layer materials we observe a strong correlation between r and $T_{c\,\max}$, which seems to be continued in the *bonding* subband for the multilayer materials (filled squares). This indicates that the electrons are delocalized over the multilayer [21], and that $T_{c\,\max}$ increases with the number of layers for the *same* reason that it increases among single-layer materials; the multilayer is simply a means of lowering ε_s further, through the formation of Cu s-Cu s bonding states. This is consistent with the celebrated pressure enhancement [22] of T_c in $HgBa_2Ca_2Cu_3O_8$ and the fact [12] that $T_{c\,\max}$ drops from 92 to 50 K when Y is replaced by the larger cation La in $YBa_2Cu_3O_7$. The r values calculated for $LaBa_2Cu_3O_7$ are included in Fig. 5 and are seen to follow the trend. That $T_{c\,\max}$ eventually drops for an increasing number of layers is presumably caused by loss of phase coherence.

Interlayer coupling in bct La_2CuO_4 mainly proceeds by hopping from O_c p_z at $(0, 0, zc)$ to its four nearest neighbors at $[\pm\frac{1}{2}, \pm\frac{1}{2}, (\frac{1}{2} - z)c]$ and is therefore taken into account by adding to $\varepsilon_{\bar{c}}$ on the right-hand side of (3) the term $-8t_{cc}^{\perp}\cos\frac{1}{2}k_x\cos\frac{1}{2}k_y\cos\frac{1}{2}ck_z$. In primitive tetragonal materials, the corresponding term is merely $\propto \cos ck_z$ because the CuO_2 layers are stacked on top of each other; the interlayer coupling in $HgBa_2CuO_4$ proceeds from O_c p_z at $(0, 0, zc)$ via Hg $6s/6p_z$ at $(0, 0, c/2)$ to O_c p_z at $[0, 0, (1 - z)c]$. Coherent interlayer coupling thus makes ε_s depend on k_z, and this passes onto the conduction band a k_z dispersion $\propto v^2\cos\frac{1}{2}k_x\cos\frac{1}{2}k_y\cos\frac{1}{2}ck_z$ in bct and $\propto v^2\cos ck_z$ in tetragonal structures. Figure 5 shows how the k_z dispersion of r decreases when the axial orbital contracts to Cu $4s$.

Our identification of an electronic parameter, r or ε_s, which correlates with the observed $T_{c\,\max}$ for all known types of hole-doped HTSC materials could be a useful

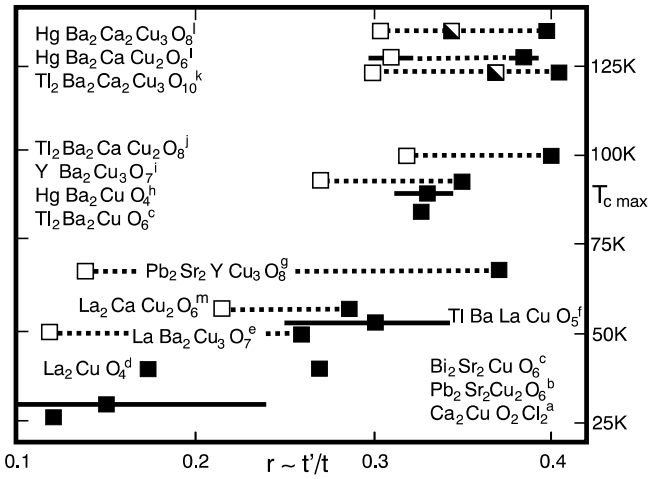

FIG. 5. Correlation between calculated r and observed $T_{c\,\max}$. Filled squares: single-layer materials and most bonding subband for multilayers. Empty squares: most antibonding subband. Half-filled squares: nonbonding subband. Dotted lines connect subband values. Bars give k_z dispersion of r in primitive tetragonal materials, $a-m$ [8–20].

guide for materials synthesis and a key to understanding HTSC. With current **k**-space renormalization-group methods one could, for instance, investigate the effect of the band shape on the leading correlation-driven instabilities [23]. Moreover, the possibility that a longer hopping range leads to better screening of the Coulomb repulsion, maybe even to overscreening, could be studied. Increased diagonal hopping, t', might lead to higher $T_{c\,\max}$ by suppression of static stripe order [24]. The Van Hove scenario [25] finds no support in Fig. 5 because it is the saddlepoint of the *antibonding* band which is at the LDA Fermi level in $YBa_2Cu_3O_7$; the bonding band is about half filled and enhances spin fluctuations with $\mathbf{q} \approx (\pi, \pi)$ [26]. The propensity to buckling is increased by pushing the conduction band towards the $O_{a/b}\ p_z$ level [4] by lowering of ε_s, but recent structural studies [12], as well as Fig. 5, disprove that static buckling enhances $T_{c\,\max}$, although dynamical buckling might. The interlayer pair-tunneling mechanism [27] is ruled out by the facts that $T_{c\,\max} \sim 90$ K in both bct $Tl_2Ba_2CuO_6$ and simple tetragonal $HgBa_2CuO_4$ although the additional factor $\cos\frac{1}{2}k_x \cos\frac{1}{2}k_y$ attained by $t^{\perp}(\mathbf{k})$ in bct materials strongly suppresses the pair tunneling. That the axial orbital is *the* channel for coupling the layer to its surroundings is supported [28] by the observations that the **k** dependence of the scattering in the normal state is v^2-like [5] and that c-axis transport is strongly suppressed by the opening of a pseudogap with similar **k** dependence [29]. The axial orbital is also *the* noncorrelated vehicle for coupling between oxygens in the layer. It therefore seems plausible that contraction of the axial orbital around the CuO_2 layer, away from the nonstoichiometric layers, will strengthen the phase coherence and thus increase $T_{c\,\max}$. Thermal excitation of nodal quasiparticles [30], on the other hand, seems not to be the mechanism by which HTSC is destroyed, because the axial orbital does not influence the band in the nodal direction. Finally, we mention that the correlation between r and $T_{c\,\max}$ does not extend to electron-doped cuprates, where the mechanism for superconductivity thus seems to be different.

Discussions with H. Beck, I. Bozovic, and Z.-X. Shen are gratefully acknowledged.

*Present address: IIT Bombay, Mumbai 400 076, India.
†Present address: S. N. Bose Centre, Calcutta 700098, India.

[1] For a recent review, see J. Orenstein and A. J. Millis, Science **288**, 468 (2000), and further articles in that volume.
[2] V. J. Emery and S. A. Kivelson, Nature (London) **374**, 434 (1995).
[3] J.-P. Locquet *et al.,* Nature (London) **394**, 453 (1998); H. Sato *et al.,* Phys. Rev. B **61**, 12 447 (2000).
[4] O. K. Andersen *et al.,* J. Phys. Chem. Solids **56**, 1573 (1995); J. Low Temp. Phys. **105**, 285 (1996).
[5] Z. X. Shen and D. S. Dessau, Phys. Rep. **253**, 1 (1995); H. H. Fretwell *et al.,* Phys. Rev. Lett. **84**, 4449 (2000); S. V. Borisenko *et al.,* Phys. Rev. Lett. **84**, 4453 (2000).
[6] O. K. Andersen *et al.,* Phys. Rev. B **62**, R16 219 (2000).
[7] I. Dasgupta *et al.* (to be published).
[8] D. N. Argyriou *et al.,* Phys. Rev. B **51**, 8434 (1995).
[9] H. W. Zandbergen *et al.,* Physica (Amsterdam) **159C**, 81 (1989).
[10] C. C. Torardi *et al.,* Phys. Rev. B **38**, 225 (1988).
[11] R. J. Cava *et al.,* Phys. Rev. B **35**, 6716 (1987).
[12] D. Goldschmidt *et al.,* Phys. Rev. B **48**, 532 (1993); O. Chmaissem *et al.,* Nature (London) **397**, 45 (1999).
[13] M. A. Subramanian *et al.,* Physica (Amsterdam) **166C**, 19 (1990).
[14] M. A. Subramanian *et al.,* Physica (Amsterdam) **157C**, 124 (1989).
[15] S. N. Putilin *et al.,* Nature (London) **362**, 226 (1993).
[16] M. A. Beno *et al.,* Appl. Phys. Lett. **51**, 57 (1987).
[17] M. A. Subramanian *et al.,* Nature (London) **332**, 420 (1988).
[18] C. C. Torardi *et al.,* Science **240**, 631 (1988).
[19] B. A. Hunter *et al.,* Physica (Amsterdam) **221C**, 1 (1994).
[20] R. J. Cava *et al.,* Physica (Amsterdam) **172C**, 138 (1990).
[21] This is consistent with the observation of bilayer splitting: D. L. Feng *et al.,* Phys. Rev. Lett. **86**, 5550 (2001); Y. D. Chuang *et al.,* cond-mat/0102386.
[22] C. W. Chu *et al.,* Nature (London) **365**, 323 (1993); M. Nunez-Regueiro *et al.,* Science **262**, 97 (1993).
[23] C. J. Halboth and W. Metzner, Phys. Rev. B **61**, 7364 (2000); C. Honerkamp *et al.,* cond-mat/9912358.
[24] M. Fleck *et al.,* cond-mat/0102041.
[25] D. M. Newns *et al.,* Comments Condens. Matter Phys. **15**, 273 (1992).
[26] V. S. Oudovenko *et al.,* Physica (Amsterdam) **336C**, 157 (2000).
[27] S. Chakravarty *et al.,* Science **261**, 337 (1993).
[28] A. Z. Zheleznyak *et al.,* Phys. Rev. B **57**, 3089 (1998); L. B. Ioffe and A. J. Millis, Phys. Rev. B **58**, 11 631 (1998).
[29] D. Basov *et al.,* Phys. Rev. B **50**, 3511 (1994); C. C. Holmes *et al.,* Physica (Amsterdam) **254C**, 265 (1995).
[30] P. A. Lee and X. G. Wen, Phys. Rev. Lett. **78**, 4111 (1997).